Biogeophysical feedback of phytoplankton on the Arctic climate. Part I: Impact of nonlinear rectification of interactive chlorophyll variability in the present-day climate

Hyung-Gyu Lim, Jong-Seong Kug & Jong-Yeon Park

Climate Dynamics
Observational, Theoretical and Computational Research on the Climate System

ISSN 0930-7575
Volume 52
Combined 9-10

Clim Dyn (2019) 52:5383-5396
DOI 10.1007/s00382-018-4450-6

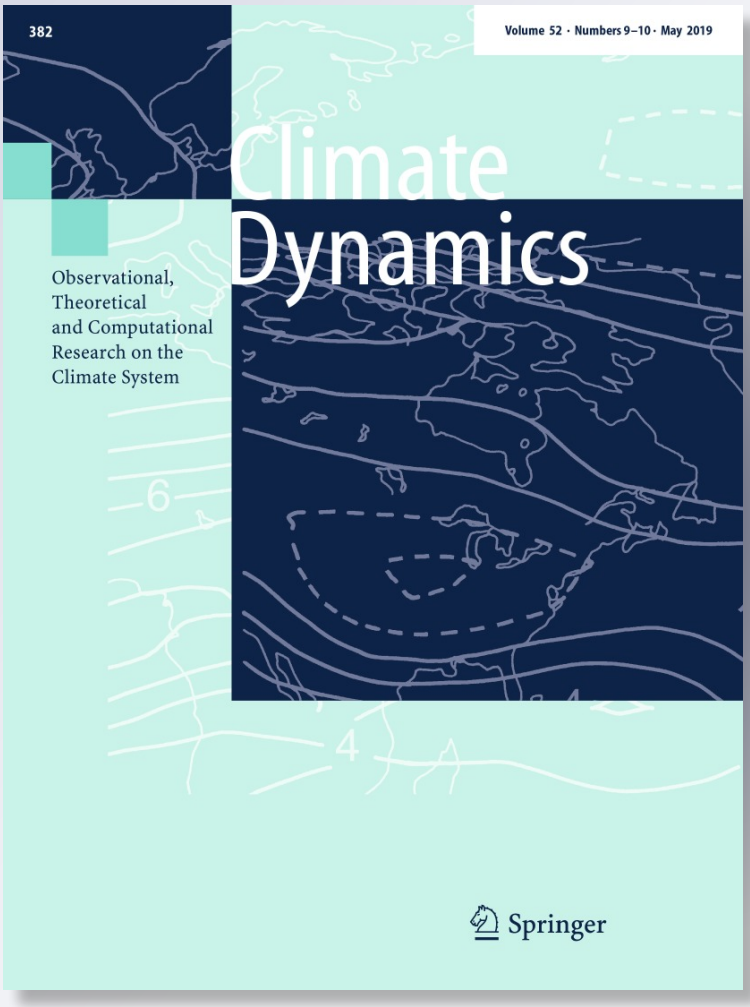

Springer

Climate Dynamics (2019) 52:5383–5396
https://doi.org/10.1007/s00382-018-4450-6

Biogeophysical feedback of phytoplankton on the Arctic climate. Part I: Impact of nonlinear rectification of interactive chlorophyll variability in the present-day climate

Hyung-Gyu Lim[1] · Jong-Seong Kug[1] · Jong-Yeon Park[2]

Received: 21 February 2018 / Accepted: 17 September 2018 / Published online: 21 September 2018

Abstract
Phytoplankton biomass substantially influences the Arctic climate via biogeophysical feedback, i.e., an increase in the mean chlorophyll concentration absorbs more shortwave radiation in the surface ocean layer, which leads to Arctic surface warming. Here, we identified that in addition to the effect of the mean chlorophyll change, an interannual chlorophyll variability substantially influences the Arctic mean climate state, even though the mean chlorophyll remains the same. We found that two nonlinear rectifications of chlorophyll variability induced Arctic cooling. One was due to the effect of a nonlinear shortwave heating term, which was induced by the positive ice–phytoplankton covariability in the boreal summer. The other was due to a cooling effect by rectification of a nonlinear function of the shortwave absorption rate, which reduced the shortwave absorption rate by interannually varying chlorophyll. In the Coupled Model Intercomparison Project, earth system models that included biogeophysical feedback simulated a colder Arctic condition than models without a biogeophysical feedback. This result suggests a possible mechanism in understanding how chlorophyll variability interacts with the Arctic climate system and its impact on the Arctic mean climate state.

Keywords Ocean biogeochemical model · Arctic climate · Chlorophyll feedback · Bio-geophysical feedback

1 Introduction

Phytoplankton pigments in the ocean absorb and use visible wavelengths of solar irradiance for photosynthesis. The solar radiation that reaches the ocean surface is exponentially absorbed by the ocean column following the e-folding depth of Beer's law (Jerlove 1968; Paulson and Simpson 1977). Phytoplankton biomass, i.e., chlorophyll, in the green ocean enhances the attenuation of solar radiation within the ocean column (Morel 1988; Morel and Antoine 1994). Therefore, the presence of chlorophyll in the green ocean induces a relatively warmer ocean surface than the absence of chlorophyll in the ocean column lacking phytoplankton (Timmermann and Jin 2002; Manizza et al. 2005; Marzeion et al. 2005). This oceanic biogeophysical feedback, the interaction between biology and ocean physics, has been investigated by a number of researchers in observations (Sathyendranath and Platt 1991; Strutton and Chavez 2004).

Biogeophysical feedback has received attention as a new parameter of the air–sea–bio interaction in climate models (Manizza et al. 2005; Marzeion et al. 2005; Lengaigne et al. 2007; Vichi et al. 2007). Earth system models (ESMs), which are interactive biogeochemical models embedded in climate models, provide several pieces of evidence of a biogeophysical effect and feedback on the global climate. Based on ESM experiments, many studies have suggested the distinctive biogeophysical impact on the global climate states (Murtugudde et al. 2002; Manizza et al. 2005; Lengaigne et al. 2007; Patara et al. 2012; Mignot et al. 2013), the El Niño–Southern Oscillation (Timmermann and Jin 2002; Marzeion et al. 2005; Lee et al. 2014; Park et al. 2014a, b; Yeh et al. 2014; Kang et al. 2017), and the Indian Ocean Dipole (Park and Kug 2013). Most of the previous studies have agreed that biogeophysical feedback affects the mean

✉ Jong-Seong Kug
jskug1@gmail.com

[1] Division of Environmental Science and Engineering, Pohang University of Science and Technology (POSTECH), 77 cheongam-Ro Nam-Gu, Pohang 790-784, South Korea

[2] Department of Earth and Environmental Sciences, Chonbuk National University, 567 Baekje-daero Deokjin-gu, Jeonju 54896, South Korea

climate states and climate variability via modulation of the shortwave heating rate on the ocean surface.

A fully coupled model study on biogeochemical processes has suggested the significant impact of biogeophysical feedback in the Arctic region (Lengaigne et al. 2009; Park et al. 2015), stating that the presence of chlorophyll induces Arctic warming (Lengaigne et al. 2009), whereas an ocean-only model study has suggested almost no impact (Manizza et al. 2005). The Arctic climate system has several positive feedbacks, such as the ice–albedo feedback (Perovich et al. 2007; Holland et al. 2010), longwave radiation by atmospheric inversion (Bintanja et al. 2011; Ding et al. 2017), and the turbulent heat flux feedback (Serreze and Francis 2006; Yim et al. 2016). Thus, the impact of biogeophysical feedback can only be understood within the coupled atmosphere–ocean context. Lengaigne et al. (2009) have suggested that the presence of Arctic chlorophyll traps the shortwave heat flux at the surface, which induces sea surface warming and reduces the sea ice concentration (SIC) and thickness. These reductions enhance a positive ice–albedo feedback to melt the sea ice.

It is suggested that under greenhouse warming, Arctic amplification due to ice–albedo feedback is enhanced by the biogeophysical feedback (Park et al. 2015). The increasing downward longwave radiation due to increased carbon dioxide melts the Arctic sea ice, allowing more solar radiation to penetrate the Arctic Ocean surface. This increase in shortwave flux enhances the positive trend of the surface phytoplankton in spring that warms the ocean surface, and future projections indicate that this will result in a faster melting of the sea ice. Thus, Arctic amplification under greenhouse warming can increase the mean chlorophyll content in the Arctic. Previous studies have provided robust results from the ESMs that the presence of chlorophyll or an increase in the mean chlorophyll concentration induces Arctic warming (Lengaigne et al. 2009; Park et al. 2015). The majority of ESMs suggested the importance of the mean chlorophyll concentration. However, the effect of interactive chlorophyll variability on the Arctic climate is not yet understood, although the biological variables are highly related to physical variables on an interannual time scale.

Arctic chlorophyll is controlled by light-limited conditions in spring (Arrigo et al. 2008; Wassmann and Reigstad 2011; Popova et al. 2012). The Arctic spring bloom is strongly dependent on the retreat of the sea ice as the Arctic sea ice plays a significant role in controlling the amount of solar radiation in the euphotic zone. The nutrient inventory in this zone is relatively sufficient for the Arctic spring bloom. Arctic sea ice growth during the boreal winter drives density-driven vertical mixing via brine rejection and an unstable vertical profile via thermodynamic cooling in the upper ocean. This vertical mixing replenishes the nutrients in the upper ocean that are preserved until spring because of few consumers during the polar night.

Arctic chlorophyll is controlled by nutrient-limited conditions in summer (Wassmann and Reigstad 2011; Arrigo et al. 2012; Popova et al. 2012). Light availability over the Arctic Ocean is relatively sufficient in summer due to the seasonal depletion of the sea ice, although nutrient availability is relatively insufficient due to the seasonal depletion of nutrients by early consumers in spring and seasonal stratification under the ice-free ocean. Thus, the summer bloom is determined by nutrient replenishment in the euphotic zone (Ardyna et al. 2014).

Variations in the Arctic sea ice is one of the dominant factors that determine the mixing of ocean layers (Peralta-Ferriz and Woodgate 2015). A high SIC enhances sunlight reflection and salinity of surface water due to brine rejection of the formation of sea ice. Thus, the seasonal stratification of the upper ocean can be reduced by the positive anomaly of the sea ice. Arrigo et al. (2012) surprisingly observed massive phytoplankton blooms beneath thick first-year sea ice in the Chukchi Sea in July, which was in contrast to a lower phytoplankton biomass in the open ocean due to nutrient depletion. This is because thinner first-year sea ice and melt ponds are increased in the boreal summer, which permits more light penetration than thicker older sea ice (Arrigo et al. 2014). These results clearly indicate that SIC is closely related to ocean stratification, which can control the phytoplankton blooms in the Arctic Ocean. Given the variability in light penetration through the sea ice, a high SIC might result in a high chlorophyll concentration in the Arctic summer due to larger nutrient concentration (Wassmann and Reigstad 2011; Bhatt et al. 2014).

Thus, the seasonal dependency of relationship between chlorophyll and sea ice is determined by seasonal limiting conditions. This study aimed to examine the interactions between chlorophyll and the Arctic climate system on an interannual time scale and to determine the impact of biogeophysical feedback of interactive chlorophyll variability on the present-day climate. To examine the impact of interactive chlorophyll variability, a pair of idealized model experiments, which were set to have the same monthly climatology of chlorophyll concentration using a Geophysical Fluid Dynamics Laboratory (GFDL)-CM2.1, were used to assess Arctic climate sensitivity. Section 2 provides a detailed description of the model experiments, and the results are presented in Sect. 3. Section 3.1 shows the general responses of the model experiments. Section 3.2 shows the impact of two nonlinear rectifications of chlorophyll variability on the Arctic mean climate state. Section 3.3 shows the relationship between the Arctic sea ice and phytoplankton in the present experiment. Lastly, Sect. 4 presents the summary and discussion.

2 Twin ESM experiments

In this study, we used a fully coupled model (version CM2.1) with the biogeochemical (BGC) model Tracers of Phytoplankton with Allometric Zooplankton version 2 (TOPAZv2) developed by GFDL (Griffies 2012; Dunne et al. 2013). This model used open source code provided by the National Oceanic and Atmospheric Administration (https://www.gfdl.noaa.gov/), which has a similar model configuration to that of Lim et al. (2017). Two different experiments were conducted using this model: (1) in the case of BGC.on, CM2.1 was integrated by turning on the BGC model for 250 years after a 550-year spin-up. Thus, chlorophyll has an interannual variability in BGC.on; (2) in the case of BGC.off, CM2.1 was integrated by turning off the BGC model for 250 years, and instead, three dimensions (longitude, latitude, and depth) for monthly climatology of chlorophyll were obtained from BGC.on and were applied to the model. Thus, chlorophyll does not have interannual variability in BGC.off. In both experiments, the atmospheric CO_2 concentration was fixed at the concentration in 1990 (353 ppm) and the mean chlorophyll concentrations were the same. Both experiments were implemented based on the same initial condition after a 550-year spin-up to avoid a long-term drift of Arctic chlorophyll and SIC. Experiment summaries are shown in Table 1. The idea behind this experimental design is that the difference between BGC.on and BGC.off demonstrates the impact of interactive chlorophyll variability by excluding the effect of mean chlorophyll change.

To investigate the biogeophysical feedback, both experiments used the same shortwave heating scheme (Manizza et al. 2005). This scheme considers the attenuation coefficients modulated by the chlorophyll concentration in horizontal and vertical grids. In detail, the fraction of the total surface irradiance between the infrared and visible wavelength bands was determined by the surface condition in an atmospheric model. Approximately 99.9% of the infrared wavelength of the total surface irradiance is absorbed in the surface 2 m of the ocean (Morel and Antoine 1994). By contrast, the visible bands of the shortwave solar radiation, partitioned between red and blue/green bands, penetrate ocean waters down to the cutoff depth (200 m in this study). In this case, the attenuation coefficients of visible bands can be determined by the vertical profile of a simulated or prescribed chlorophyll concentration. This scheme considers the self-shading effect, i.e., the shortwave heating of the deeper ocean layer is affected by the chlorophyll concentration in the upper layer that absorbs the shortwave radiation first. This scheme allows for the computation of the biogeophysical feedback in every integration time and at the global scale in CM2.1.

We evaluated the simulated chlorophyll concentration in BGC.on by comparing it to climate observations from 1998 to 2004 of the European Space Agency Ocean Colour Climate Change Initiative project (ESA-CCI, version 3), which is available online at http://www.esa-oceancolour-cci.org/ (Müller et al. 2015). Based on the satellite-retrieved data, the simulated chlorophyll concentrations in BGC.on averaged from 20 m to the surface, showing a pattern similar to that in the tropics (high) and subtropics (low) (Fig. 1a, b), which is consistent with the GFDL ESM2M results (Dunne et al. 2013). TOPAZv2, the marine biogeochemical model used for this study, is a good model with the highest global spatial correlation skill score of 0.72 and a relatively low global mean bias of 0.04 mg/m^3 among the biogeochemical models embedded in the fifth phase of the Coupled Model Intercomparison Project (CMIP5) (Laufkötter et al. 2015). In the Arctic, the pattern of a high chlorophyll concentration in the Bering Strait, Chukchi Sea, and the Barents Sea and a low concentration in the center of the Arctic is also similar to the satellite-retrieved data. However, the simulated chlorophyll has a lower mean concentration in the boreal summer than in the satellite observation. Nevertheless, BGC.on simulates a realistic seasonal cycle of Arctic chlorophyll concentrations in ice-free conditions, i.e., it shows double peaks (Wassmann and Reigstad 2011; Ardyna et al. 2014) (Fig. 1c). Therefore, GFDL-CM2.1 is useful to investigate the coupling process of air–sea–bio interactions and its impact on the Arctic climate.

3 Results

3.1 Impact of interactive chlorophyll variability

In general, interactive chlorophyll variability leads to cooling in the Arctic mean climate states. Figure 2 shows the difference in the mean states between BGC.on and BGC.off experiments. Figure 2a shows the significant difference of sea surface temperature (SST), SIC, and surface temperature in the Arctic region. The SST in BGC.on averaged from May to October and is cooler overall about −0.11 °C than that in

Table 1 Summary of the experiments used in this study

Exp.	Model	Chlorophyll concentration	Simulated period
BGC.on	CM2.1 + TOPAZ2	Simulated chlorophyll	250 years after 550-year spin-up
BGC.off	CM2.1	Monthly climatology of chlorophyll in BGC.on on global scale	250 years after 550-year spin-up

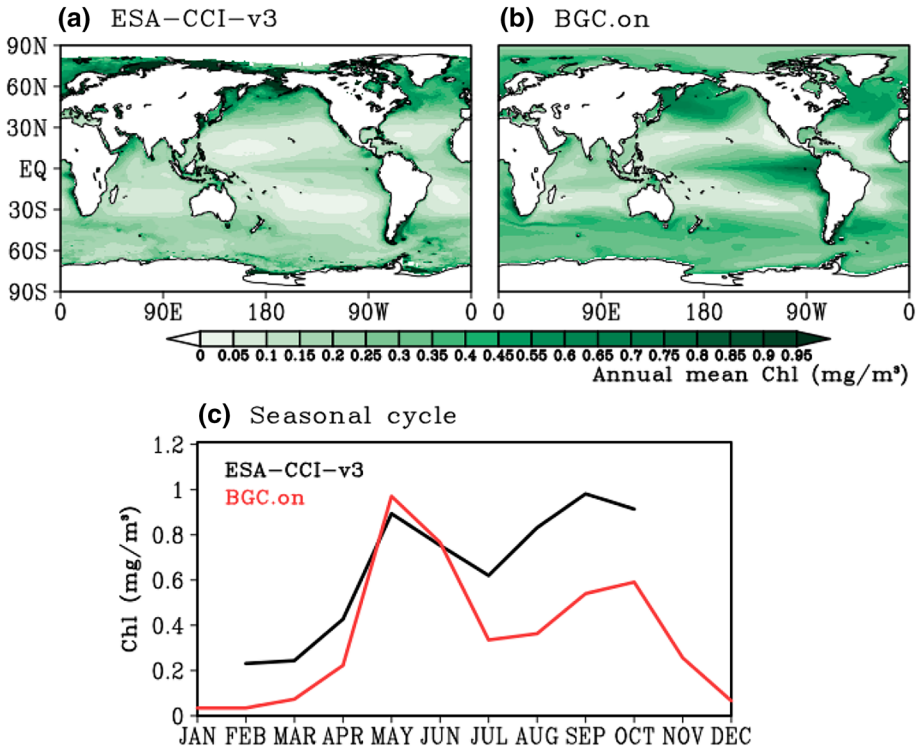

Fig. 1 Mean annual surface chlorophyll concentration in **a** ESA-CCI-v3 and **b** BGC.on (> 20 m). **c** Seasonal cycle of Arctic chlorophyll concentration (> 65°N) over the ice-free condition [< 15% SIC based on HadISST (Rayner et al. 2003) and < 15% SIC based on BGC.on]

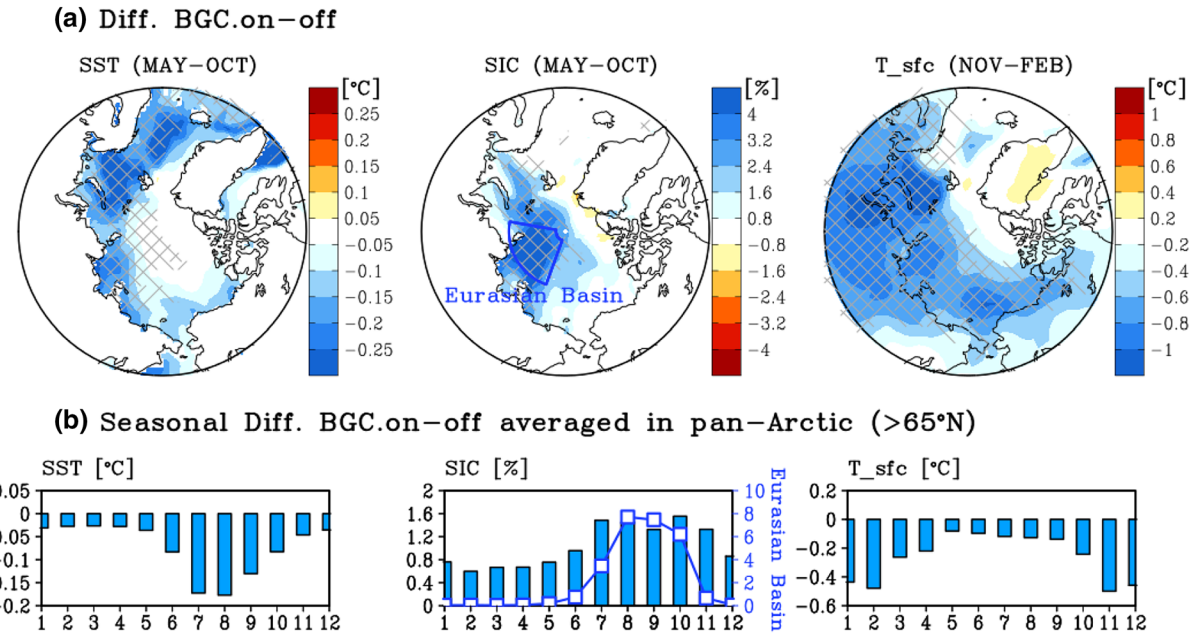

Fig. 2 The colder conditions of the Arctic in BGC.on induced by chlorophyll interannual variability than that in BGC.off. **a** The upper panels show the difference between BGC.on and BGC.off (95% statistically significant; hatched area) of sea surface temperature (SST) and sea ice concentration (SIC) from May to October and surface temperature (T_sfc) from November to February. **b** The bottom panels show the same information as **a** but is seasonal differences averaged in the Arctic region (> 65°N; bars) and is the index area of the Eurasian Basin (blue line)

BGC.off in the Arctic Ocean. The SIC in BGC.on averaged from May to October is also higher about 1.25% than that in BGC.off in the Arctic Ocean. In particular, the SIC differences are distinctive near Laptev, Kara, and the Barents Sea (hereafter referred to as the Eurasian Basin, 80°–160°E, 78°–88°N). Furthermore, a higher SIC enhances the downward reflection

of the shortwave radiation due to a high albedo, which in turn leads to a decrease in the surface temperature during winter (November–February) about −0.48 °C over pan-Arctic. This indicates that the interactive chlorophyll variability plays a role in increasing the sea ice and decreasing the temperature. These cold conditions in BGC.on over the pan-Arctic (averaged > 65°N) are clear for whole months (Fig. 2b). The maximum SIC response (approximately + 8%) in the Eurasian Basin appeared in August (blue line in Fig. 2b).

The colder condition in BGC.on than those in BGC.off is related to a decrease in the shortwave heating on the Arctic Ocean surface. The difference in the shortwave heating in the upper ocean (0–30 m) between the two experiments shows a negative pattern in the pan-Arctic (Fig. 3a). In particular, the shortwave heating in August was distinctively decreased by an average of approximately 13% (−5.58 W/m^2) in the Eurasian Basin (Fig. 3b) where the SIC changes are the largest. Compared to the prescribed chlorophyll simulation (BGC.off), the interactive chlorophyll simulation (BGC.on) shows significantly less shortwave heating. This less heating will induce decrease in SST and increase in Sea ice. Although the cooling effect of the Arctic Ocean by the interactive chlorophyll variability might be initially small, it can be amplified by a strong positive sea ice–albedo feedback, which induces significant differences in SST and sea ice as shown in Fig. 2. Hence, the interannual chlorophyll variability significantly influences the cold Arctic condition eventually.

3.2 Two nonlinear rectifications of chlorophyll variability on the Arctic mean climate state

We showed that the interactive chlorophyll variability has a significant cooling effect on the Arctic mean climate state because the shortwave flux is less absorbed when chlorophyll varies in interannual timescale. Here, we offer suggestions as to why a reduced absorption of the shortwave flux occurs when chlorophyll varies compared with when it does not.

To address the effect of chlorophyll variability, we first need to define the shortwave absorption rate (α_{sw}). Shortwave heating is controlled by the multiplication of the shortwave flux (swflx) reaching the ocean and its absorption rate in the ocean interior. Therefore, α_{sw} can be simply calculated by the shortwave heating divided by the shortwave flux. Then, α_{sw} variability is a function of chlorophyll variability that is positively correlated (by approximately 0.82–0.95) over most seasons when solar radiation is available. To quantify the surface shortwave heating, α_{sw} and the shortwave heating were integrated over 30 m.

The shortwave heating difference between BGC.on and BGC.off (Fig. 3) can be represented by the difference in the time mean of shortwave heating (MSH) as $\overline{\alpha_{sw} \times swflx}$. The difference in MSH (i.e., $\overline{\alpha_{sw} \times swflx}$) between BGC.on and

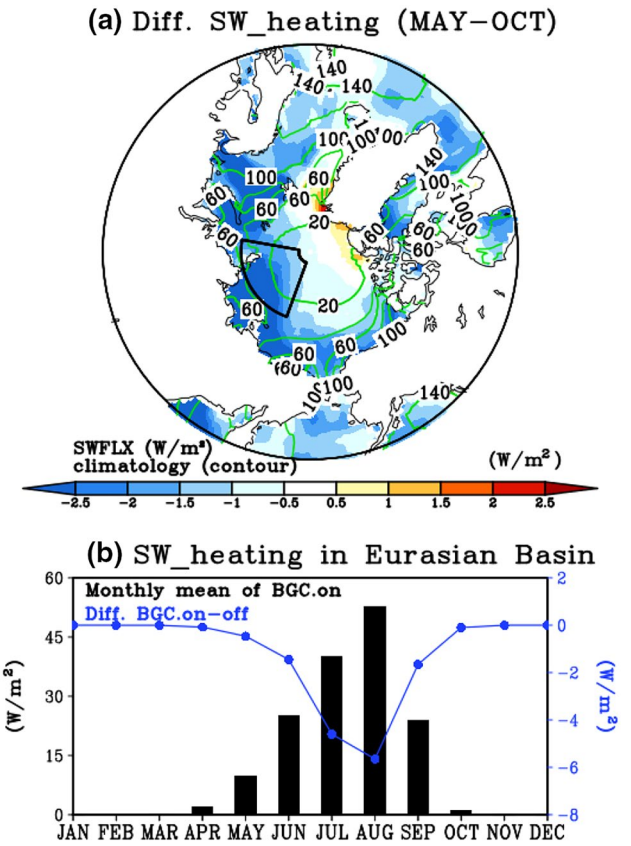

Fig. 3 The less shortwave heating in BGC.on is induced by chlorophyll interannual variability than that in BGC.off. **a** The shortwave heating (SW_heating) difference between BGC.on and BGC.off (shading) and the climatological mean shortwave flux into the ocean of BGC.on (SWFLX, contour) averaged from May to October in the upper 30 m of the ocean. **b** The Eurasian Basin (80°–160°E, 78°–88°N) climate monthly mean shortwave heating in BGC.on (black bar) and the difference in the shortwave heating between BGC.on and BGC.off (blue line)

BGC.off shows strong cooling in the Eurasian Basin (blue in Fig. 3b) due to the combined result of the impact of the interactive chlorophyll variability and the responses to increased SIC (blue in Fig. 2b) via the positive feedbacks. Thus, further division of the MSH is essential to understand how the interactive chlorophyll variability initially rectifies the cold Arctic condition.

The α_{sw} can be divided by the mean term $\overline{\alpha_{sw}}$, the monthly α_{sw} mean, and the interannual variability term α'_{sw}, the monthly α_{sw} anomaly. The shortwave flux can also be divided by the mean term $\overline{swflx}$, the monthly shortwave flux mean, and the interannual variability term $swflx'$, the monthly shortwave flux anomaly. Thus, the MSH can be divided into two terms as follows:

$$\overline{\alpha_{sw} \times swflx} = \overline{\overline{\alpha_{sw}} \times \overline{swflx}} + \overline{\alpha'_{sw} \times swflx'}$$

where $\overline{\alpha_{sw}} \times \overline{swflx}$ is the mean of MSH (MMSH) and $\overline{\alpha'_{sw} \times swflx'}$ is the mean of the nonlinear shortwave heating (MNSH).

When using the MMSH and MNSH terms, we found two nonlinear rectifications of the interactive chlorophyll variability. First, we investigated the MNSH term and noted that it was almost zero in BGC.off because α_{sw} did not vary temporally due to the prescribed chlorophyll concentration. We computed the MNSH in the upper ocean to up to 30 m using BGC.on output. This term clearly shows an overall negative pattern in August over the pan-Arctic (Fig. 4a), indicating the summer shortwave cooling effect. In the Eurasian Basin, this cooling signal is strongest in July and August (Fig. 4b).

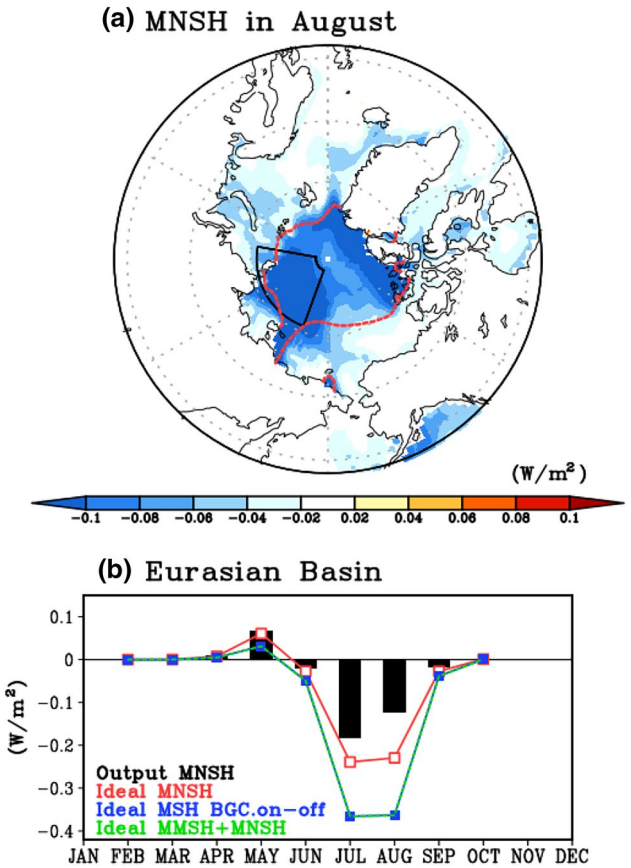

Fig. 4 Two nonlinear rectification effects induce the summer shortwave cooling. **a** August output of the mean nonlinear shortwave heating term (MNSH) $\alpha'_{sw} \times swflx'$ up to 30 m in BGC.on. The climatological sea ice edge (15%) in BGC.on in August (red dashed line) and index area of the Eurasian Basin (80°–160°E, 78°–88°N; black sector). **b** The Eurasian Basin monthly MNSH $\overline{\alpha'_{sw} \times swflx'}$ in the BGC.on output (bar) and the ideal BGC.on (red line). The difference in the mean shortwave heating term (MSH) $\overline{\alpha_{sw} \times swflx}$ between the ideal BGC.on and BGC.off (blue line). $\Delta\overline{\alpha_{sw} \times swflx}$ (Δ is BGC.on minus BGC.off) plus the ideal MNSH of BGC.on (green line). The blue and green lines are perfectly overlapped

In BGC.on, the summer cooling effect of the MNSH can be simply determined by the covariance between the anomalous shortwave flux and chlorophyll concentration because chlorophyll variability controls α'_{sw}. Figure 5a shows the strong negative covariance coefficient between chlorophyll concentration and shortwave flux in summer that is similar to the MNSH in the Eurasian Basin (Fig. 4b). Shortwave flux is mostly determined by the surface condition, and in the Arctic, shortwave flux reflectivity is controlled by the SIC variability due to the high albedo of the sea ice. Hence, the covariance between the SIC and the shortwave flux has an opposite but similar pattern to the covariance between the SIC and chlorophyll (Fig. 5b).

The summer shortwave cooling effect by the MNSH can be explained by the physical interaction between the SIC and the chlorophyll variabilities. The summer chlorophyll concentration is determined by nutrient availability (Carmack et al. 2006; Arrigo et al. 2008; Wassmann and Reigstad

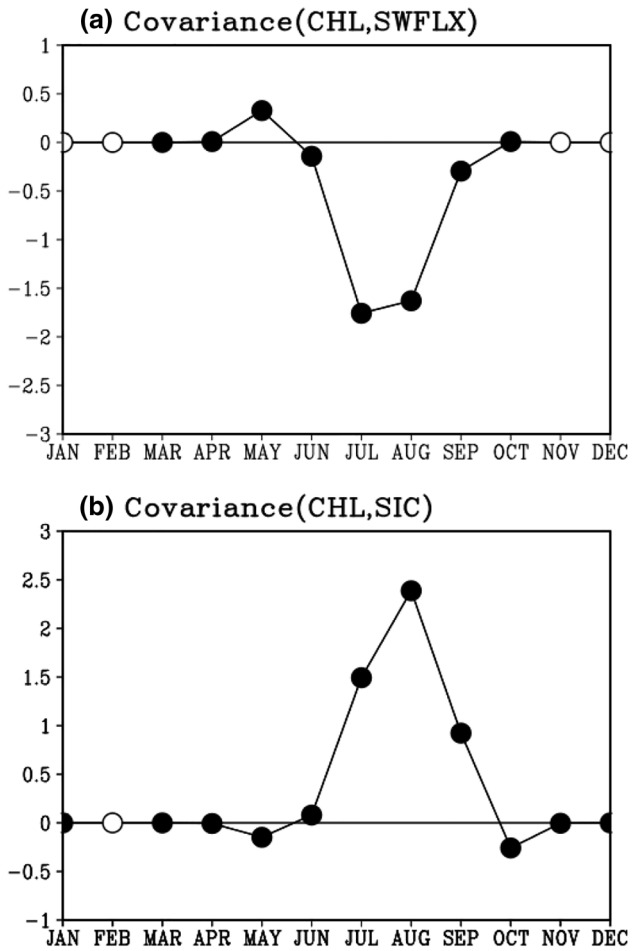

Fig. 5 Simultaneous covariance coefficients between **a** chlorophyll and the shortwave flux as well as **b** chlorophyll and sea ice concentration (SIC) in the Eurasian Basin (80°–160°E, 78°–88°N). The closed circles denote significance at 95%

2011; Ardyna et al. 2014; Bhatt et al. 2014). The Arctic sea ice is one of the dominant factors that drive ocean mixing due to thermodynamic cooling on the ocean surface via the reflection of the shortwave radiation and dense sea water caused by brine rejection near sea ice formations (Cabré et al. 2015; Peralta-Ferriz and Woodgate 2015). Thus, enhanced ocean mixing in high SIC conditions leads to chlorophyll growth in summer, which explains the positive relationship between the SIC and chlorophyll variabilities in summer. This positive ice–phytoplankton relationship leads to a negative covariance between the shortwave flux and chlorophyll in summer, and it is a key factor for the summer shortwave cooling by the MNSH. Section 3.3 provides a detailed analysis of nutrient and ocean mixing mechanisms related to the SIC and the chlorophyll variability.

The ideal MNSH term precisely supports the summer shortwave cooling effect (Fig. 4b). The shortwave heating scheme designed by Manizza et al. (2005) is a function of four variables: shortwave flux, chlorophyll concentration, visible fraction of the shortwave flux, and ocean thickness. To identify shortwave heating that is affected by chlorophyll variability alone, the ideal MNSH was calculated using the monthly mean chlorophyll and the shortwave flux in BGC.on. However, in this calculation, other variables, such as the visible fraction of the shortwave flux and the ocean thickness, were prescribed by a climatological value in BGC.on. This recalculated MNSH shows shortwave cooling in summer (Fig. 4b), which is similar to the direct MNSH calculation (Fig. 4b). Therefore, the summer shortwave cooling effect calculated by the MNSH can be mostly attributed to chlorophyll and the shortwave flux covariability. Hereafter, this summer cooling effect by the MNSH will be referred to as Arctic cooling by the rectification of a nonlinear term of shortwave heating (NT_{sw}).

Although cooling by the rectification of NT_{sw} considerably explains the Arctic cooling effect, a sizable portion remains unexplained. The ideal MSH ($\overline{\alpha_{sw} \times swflx}$) for BGC.on was estimated based on the monthly mean shortwave flux and the chlorophyll data in BGC.on, and it represents the net effect of interactive chlorophyll variability without a mean change in the shortwave flux via the increased sea ice and its positive feedback. The difference in the ideal MSH between BGC.on and BGC.off manifests as a cooling effect (Fig. 4b) that is cooler than the cooling effect by the rectification of NT_{sw} (Fig. 4b). This suggests that another mechanism that induces the cooling effect exists in the MMSH ($\overline{\alpha_{sw}} \times \overline{swflx}$).

Second, we found that cooling by the rectification of the nonlinear function of the shortwave absorption rate (NF_{α}) was in the shortwave heating equation itself. Following Beer's law, the shortwave absorption rate is exponentially attenuated by an e-folding depth (Jerlove 1968; Paulson and Simpson 1977). Because the absorption rate (α_{sw}) is approximately determined by an exponential function of chlorophyll ($1 - \exp^{-[chl]}$, Eq. 5 in Manizza et al. 2005), the change in α_{sw} corresponding to the changing chlorophyll is nonlinear (Fig. 6), which represents a decaying slope of α_{sw} against the increasing chlorophyll. This α_{sw} nonlinearity indicates that the absorption rate response to a positive chlorophyll anomaly is smaller than the responses to a negative chlorophyll anomaly. Given that the chlorophyll concentration is fixed in BGC.off, the mean time of the absorption rate $\overline{\alpha_{sw}}$ in BGC.on is always smaller than that in BGC.off. As such, $\Delta\overline{\alpha_{sw}}$ (i.e., the difference in $\overline{\alpha_{sw}}$ between BGC.on and BGC.off) is always negative. This implies that the ocean surface absorbs less shortwave radiation due to the temporal variation in chlorophyll concentration.

Consequently, the cooling effect of the interactive chlorophyll variability and the difference in the ideal MSH between BGC.on and BGC.off can be mostly explained by adding the two terms $\Delta\overline{\alpha_{sw}} \times \overline{swflx}$ and $\overline{\alpha'_{sw} \times swflx'}$ in all months (Fig. 4b), i.e., these two rectifications of NT_{sw} and NF_{α} are essential to induce a colder Arctic condition by the interactive chlorophyll variability in BGC.on.

3.3 Relationship between the Arctic sea ice and phytoplankton

In the previous section, we showed that the interactive chlorophyll variability leads to cooling over the Arctic by two nonlinear rectification effects. One is associated with the

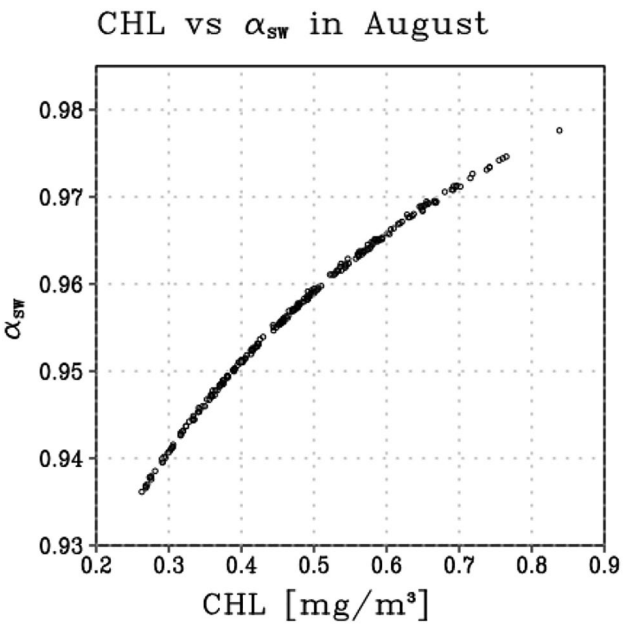

Fig. 6 Scatter diagram of the idealized α_{sw} in BGC.on with chlorophyll concentration based on the Eurasian Basin index in August. In this ideal case, calculation of α_{sw} is based on chlorophyll interannual variability in BGC.on. The other factors, visible fraction in shortwave flux (0.59) and column thickness of the surface (9.14 m) and subsurface (10 m), were fixed as climatologies of BGC.on

rectification of NF_{α} (i.e., a nonlinear function of the shortwave absorption rate) based on the exponential decay function of Beer's law. The other is associated with the rectification of NT_{sw} (i.e., a nonlinear term of shortwave heating), which is strongly associated with the covariability between chlorophyll and the shortwave flux. In this subsection, we will examine the dynamic processes of this covariability and its seasonal dependency.

In spring [March–May (MAM)], chlorophyll variability is strongly related to the shortwave flux variability, which is positively correlated (0.68–0.75) in the Eurasian Basin (Fig. 7). Light availability determines the spring chlorophyll variability because a rich nutrient inventory through the polar winter is preserved until the Arctic spring bloom. This explains the positive correlation between the shortwave flux and chlorophyll. The negative correlation of the SIC and chlorophyll (Fig. 7) (correlation coefficients from −0.68 to −0.72 in the Eurasian Basin) can be understood in the same context. The shortwave flux is associated with the surface albedo; a high SIC reflects more shortwave flux than a low SIC (Fig. 7). Thus, the chlorophyll variability is negatively correlated with SIC.

In summer [July–September (JAS)], the chlorophyll variability is also strongly related to the shortwave flux variability, although it is negatively correlated (from −0.84 to −0.91) in the Eurasian Basin (Fig. 7). In this season, nutrient variability determines the chlorophyll variability. The sunlight is relatively sufficient for phytoplankton growth in summer when the SIC is at a minimum and the sun is at its highest zenith angle. However, a seasonally depleted nutrient inventory by early consumers (i.e., spring chlorophyll) and a stabilized ocean due to the seasonal retreat of sea ice induce a nutrient-limited condition for chlorophyll. Under this condition, a chlorophyll bloom is dependent on the variability of nutrient supply in the euphotic zone that is determined by a sea ice variability. A high SIC anomaly reflects the anomalous shortwave flux input, which reduces the anomalous surface warming and the ocean stability. In addition, the anomalous positive SIC condition increases the density of surface seawater by freezing the fresh water, which reduces the ocean stability, that could enhance the vertical mixing of the Arctic ocean. Thus, the chlorophyll variability is positively correlated with SIC variability (correlation coefficients of 0.75–0.89) in the Eurasian Basin. Therefore, the variations in chlorophyll and SIC are strongly linked during the Arctic spring and summer, and SIC controls chlorophyll variability via dynamic processes (hereafter, ice–phytoplankton coupling).

An increasing SIC and a deeper mixed layer depth (MLD) affect chlorophyll variability in summer. We investigated the seasonal factors that affect the chlorophyll variability in summer. In the Eurasian Basin, lead–lag correlations of chlorophyll in JAS were calculated against a sliding average of the seasonal MLD, SIC, nitrate (NO_3), and chlorophyll (Fig. 8). The chlorophyll in JAS was positively correlated with the SIC and NO_3 in all seasons. This implies that a higher SIC supports a higher chlorophyll concentration in JAS. In addition, a higher NO_3 results in a higher chlorophyll concentration, which indicates that the Arctic summer is associated with a nutrient-limited condition. The chlorophyll in JAS is also affected by the chlorophyll in MAM. Under a high SIC condition, less nutrient consumption by the decreased chlorophyll in spring facilitates chlorophyll

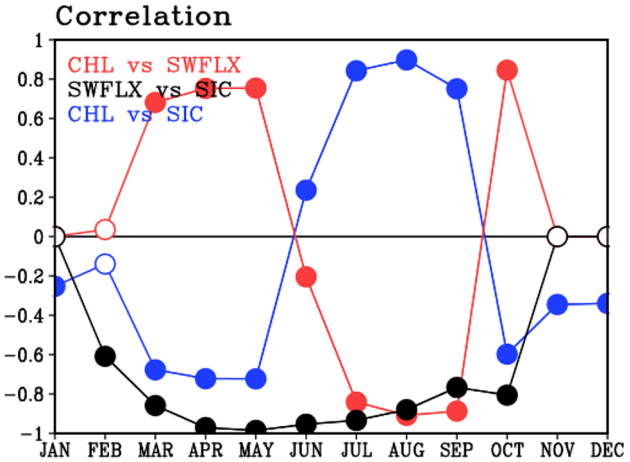

Fig. 7 Simultaneous correlation coefficients in the Eurasian Basin (80°–160°E, 78°–88°N). Simultaneous monthly correlations between the shortwave flux into the ocean (SWFLX) and chlorophyll (CHL; red), between SWFLX and sea ice concentration (SIC; black), and between chlorophyll concentration (CHL) and SIC (blue). The closed circles denote significance at 95%

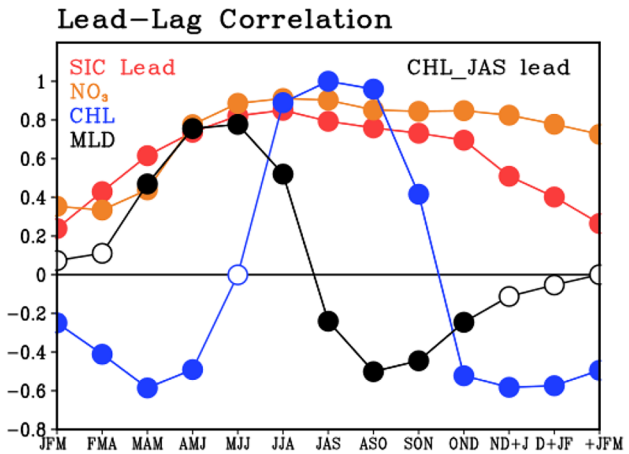

Fig. 8 Lead–lag correlation coefficients of the anomalous chlorophyll averaged from July to September (JAS) in the Eurasian Basin (80°–160°E, 78°–88°N) against a sliding average of the seasonal variables such as sea ice concentration (SIC; red), nitrate (NO_3; orange), chlorophyll concentration (CHL; blue), and mixed layer depth (MLD; black). The closed circles denote significance at 95%

growth in summer. The deeper MLD from May to July leads to an increase in the chlorophyll concentration in JAS.

After that, an increase in chlorophyll concentration in JAS leads to MLD shoaling 1 month later (i.e., from August to October). The increased chlorophyll can absorb more shortwave flux on the ocean surface via biogeophysical feedback, and this process might contribute to the re-stratification of the ocean surface (Peralta-Ferriz and Woodgate 2015).

Ice–phytoplankton coupling is strongly dependent on season due to the different limiting conditions of light and nutrients. In summer, a positive correlation between chlorophyll and SIC is explained by coupling between the sea ice formation and ocean mixing. This positive relationship leads to the seasonality of the shortwave flux and chlorophyll covariability. Note that the shortwave flux and chlorophyll variabilities are stronger in summer than in spring (Table 2), leading to a stronger summer covariance coefficients as shown in Fig. 5. Ice–phytoplankton coupling is key to explaining the physical process of the Arctic summer cooling by the rectification of NT_{SW}.

4 Summary and discussion

Previous studies on the Arctic biogeophysical feedback using ESMs (Lengaigne et al. 2009; Park et al. 2015) have provided robust results that the presence of chlorophyll or increasing mean chlorophyll concentration induces Arctic warming. The majority of ESMs suggested mechanisms that highlighted the impact of a mean chlorophyll state. However, the effect of the interactive chlorophyll variability, which is highly related to the physical variables on an interannual time scale, on the Arctic climate is firstly examined in this study. We examined the impact of the interactive chlorophyll variability based on GFDL-CM2.1 in the present-day climate. The approach of sensitivity experiments over long-term integrations showed that the interactive chlorophyll variability plays a role in cooling over the Arctic. Two nonlinear rectification effects and their mechanisms are suggested to explain the cooling effect of chlorophyll variability. Here, we summarize our major findings.

Table 2 Standard deviation in the mean chlorophyll concentration and shortwave flux in BGC.on in the Arctic over 65°N and the Eurasian Basin (80°–160°E, 78°–88°N)

Month	Standard deviation of chlorophyll concentration (10^{-2} mg/m^3)		Standard deviation of shortwave flux (W/m^2)	
	Arctic	Eurasian Basin	Arctic	Eurasian Basin
March	0.32	0.12	0.65	0.07
April	1.35	1.89	1.93	0.59
May	4.17	11.64	4.73	3.75
June	4.11	9.15	7.11	7.67
July	4.53	15.67	7.36	13.35
August	3.32	12.28	5.20	14.68

- The interactive chlorophyll experiment simulates the Arctic mean cooling state, i.e., it simulates significantly higher SIC over the pan-Arctic region, which is maximized about + 8% in the Eurasian Basin appeared in August, and lower surface temperature about − 0.48 °C over the pan-Arctic region in winter (November–February) than the non-interactive chlorophyll experiment.
- Mechanism 1 is the rectification of the NT_{sw}: the MNSH term $\overline{\alpha'_{sw} \times swflx'}$ is negative in summer. This is because chlorophyll variability controls $\alpha_{sw}{}'$ and the negative covariance between anomalous shortwave flux and chlorophyll in summer, which results in a cooling effect by the rectification of the NT_{sw}. The process of the sea ice affecting chlorophyll variability explains the summer shortwave cooling effect of NT_{sw}. Ocean mixing is enhanced by the sea ice due to thermodynamic cooling on the ocean surface due to the reflection of shortwave radiation and dense sea water caused by brine rejection near sea ice formation. The enhanced ocean mixing under a high SIC condition leads to chlorophyll growth in the nutrient-limited conditions of the Arctic summer. At the same time, a reduced shortwave flux under a high SIC condition corresponds to a negative covariability between the shortwave flux and chlorophyll. Thus, the SIC variability is key for explaining the mechanism of the summer shortwave cooling effect of NT_{sw}.
- Mechanism 2 is the rectification of the NF_{α}: the shortwave absorption rate (α_{sw}) against chlorophyll increase is followed by the e-folding depth of shortwave attenuation ($1 - \exp^{-[chl]}$), i.e., the change in α_{sw} is nonlinear, a decaying slope of α_{sw}, against increasing chlorophyll. Given that the chlorophyll concentration is fixed, the mean time of the shortwave absorption rate ($\overline{\alpha_{sw}}$) in the case of existing chlorophyll variability is always smaller than $\overline{\alpha_{sw}}$ in the case of fixed chlorophyll concentration. It generates $\Delta\overline{\alpha_{sw}}$ in the presence of chlorophyll variability, i.e., it is always negative. This implies that the cooling effect of the rectification by NF_{α} is due to temporal variation in chlorophyll.

This study is an initial assessment that attempted to quantify the cooling effect of the interactive chlorophyll variability based on single model results. Lengaigne et al. (2009) pioneered the idea of Arctic warming impact of interactive chlorophyll using the Institut Pierre Simon Laplace (IPSL)-CM4 model and reported that the interpretation was limited to the major impact of the mean chlorophyll difference. This warming impact might be partly underestimated under SIC

reduction and SST warming due to the cooling impact of chlorophyll variability.

The suggested mechanisms of the shortwave cooling by the interactive chlorophyll variability may also work in the other models. To check this possibility, we analyzed 43 climate simulations from CMIP5 archives. Among the 43 simulations, seven models considered biogeochemical processes, including chlorophyll-based shortwave penetration schemes, most of which were based on a chlorophyll-based parameterization of Morel (1988) and Beer's law. To roughly examine the effect of interactive chlorophyll variation, we separated the seven models (turned on biogeophysical feedback; the BGP.on group) from the others (turned off biogeophysical feedback; the BGP.off group), as listed in Table 3.

Interestingly, the BGP.on group showed a strong negative covariance between chlorophyll and the shortwave flux (Fig. 9a). In addition, this group showed overall positive covariance coefficients between SIC and chlorophyll in summer (Fig. 9b). These covariabilities are similar to the results in this experiment (Fig. 5). Thus, it is suggested that ice–phytoplankton coupling and chlorophyll variability lead to cooling via rectification effects of NT_{sw} and NT_{α} in the Arctic and that the interactive chlorophyll variability in the BGP.on group may simulate a colder Arctic climate than BGP.off group.

We analyzed the SIC bias averaged over JAS of the multi-model ensemble of the BGP.off group (Fig. 10). The ensemble mean of the BGC.off group tended to simulate less SIC compared with Hadley Center Sea Ice and Sea Surface Temperature (HadISST) (Rayner et al. 2003) sea ice observation data over the center of the Arctic region (Fig. 10a). Interestingly, although BGP.on group includes the presence of chlorophyll and chlorophyll interannual variability, ensemble mean of the BGP.on group tends to simulate a higher SIC in the Arctic than that of the BGC.off group (Fig. 10b). Figure 10c shows the Arctic sea ice evolution in individual models. The multi-model ensemble mean of all CMIP5 models tends to simulate the underestimated SIC in the Arctic, which is consistent to previous report of underestimated the summer sea ice in CMIP5 models (Stroeve et al. 2012). Although there is the strong diversity in simulating the Arctic sea ice, most of the BGC.on models

Table 3 CMIP5 ESMs and CGCMs used in this study

Group of turning on biogeophysical feedback (BGP.on) in CMIP5 ESMs	
1. GFDL-ESM2G (Manizza et al. 2005; Dunne et al. 2012; Griffies 2012)	
2. GFDL-ESM2M (Manizza et al. 2005; Dunne et al. 2012; Griffies 2012)	
3. IPSL-CM5A-LR (Lengaigne et al. 2007; Dufresne et al. 2013; Mignot et al. 2013)	
4. IPSL-CM5A-MR (Lengaigne et al. 2007; Dufresne et al. 2013; Mignot et al. 2013)	
5. IPSL-CM5B-LR (Lengaigne et al. 2007; Dufresne et al. 2013; Mignot et al. 2013)	
6. CESM1-BGC (Ohlmann 2003; Jochum et al. 2010; Lindsay et al. 2014)	
7. CMCC-CESM (Vichi et al. 2007; Patara et al. 2012)	
Group of turning off biogeophysical feedback (BGP.off) in CMIP5 ESMs (bold) and CGCMs	
8. CNRM-CM5	26. FGOALS-g2
9. MPI-ESM-LR	27. FIO-ESM
10. MPI-ESM-MR	28. GFDL-CM2p1
11. MRI-ESM1	29. GFDL-CM3
12. GISS-E2-H-CC	30. GISS-E2-H
13. CanESM2	31. GISS-E2-R
14. HadGEM2-CC	32. HadCM3
15. HadGEM2-ES	33. HadGEM2-AO
16. GISS-E2-R-CC	34. HadGEM2-CC
17. ACCESS1-0	35. HadGEM2-ES
18. ACCESS1-3	36. inmcm4
19. bcc-csm1-1	37. MIROC4h
20. CanCM4	38. MIROC5
21. CCSM4	39. MIROC-ESM-CHEM
22. CMCC-CM	40. MPI-ESM-P
23. CMCC-CMS	41. MRI-CGCM3
24. CSIRO-Mk3-6-0	42. NorESM1-ME
25. EC-EARTH	43. NorESM1-M

The biogeophysical ESM scheme references are provided in parenthesis for the BGP.on group

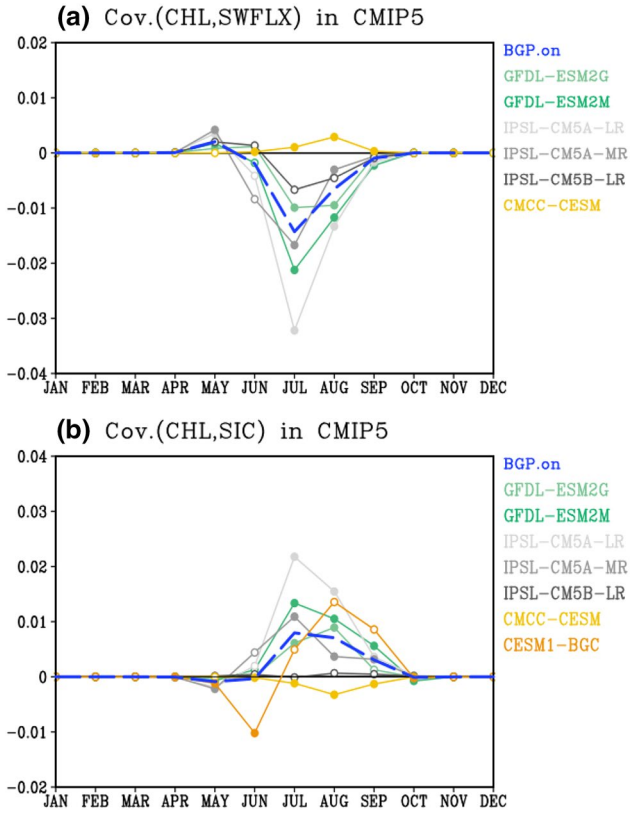

Fig. 9 Simultaneous covariance coefficients of **a** net downward shortwave radiation at the sea water surface (SWFLX) and **b** sea ice concentration (SIC) against the chlorophyll of a multi-model ensemble mean (MME) in BGP.on group of CMIP5 (dashed blue) and individual models in the Eurasian Basin (80°–160°E, 78°–88°N) from 1980 to 2004. The closed circles denote significance at 95%. BGP.on group in CMIP5 is as described in Table 3

simulate a higher SIC than the multi-model averages of the BGC.off models, except the IPSL-CM5A-MR model. This result suggests a possibility that allowing ice–phytoplankton coupling and biogeophysical feedback affect mean climate in the Arctic as suggested in this study. However, more careful analyses and modeling efforts will be necessary to quantify the role of the biological feedback in Arctic mean climate.

It was reported that a massive phytoplankton bloom occurs beneath the pack sea ice in summer at a concentration of almost 100% (Arrigo et al. 2012). This is because a thinning sea ice and the increasing number of melt ponds allow shortwave penetration through the sea ice, which enhances light availability. The sub-ice ocean provides active density-driven vertical ocean mixing via brine rejection and an unstable vertical profile due to thermodynamic cooling in the upper ocean. Hence, the sub-ice ocean has a relatively sufficient nutrient inventory compared with that of the open ocean water. This sub-ice phytoplankton has been estimated to have increased over the last decade by nearly 30% from that observed 20 years ago (Horvat et al. 2017). In other words, the positive relationship of ice–phytoplankton coupling in summer is amplified today. It should be assessed further to refine the summer shortwave cooling effect in the Arctic climate by adding the sea ice parameters of melt ponds and its radiative transmission.

Based on the long-term future projection, an ice-free condition in September is predicted as likely to occur (Boé et al. 2009). Corresponding to the decline in the sea ice, strong stratification and nutrient depletion are projected as likely in the Arctic under greenhouse warming (Vancoppenolle et al. 2013; Cabré et al. 2015). Park et al. (2015) reported that the amplified Arctic warming by an increase in the mean chlorophyll under greenhouse warming results from assuming the equal impacts of the chlorophyll variability in the present-day and future climate. Thus, it is expected that the ice–phytoplankton coupling will change according to the vanishing sea ice and nutrient inventory in the future climate. The change in ice–phytoplankton coupling provides a feedback for the climate mean state, which affects Arctic amplification under greenhouse warming. This feedback will be examined further in a future study.

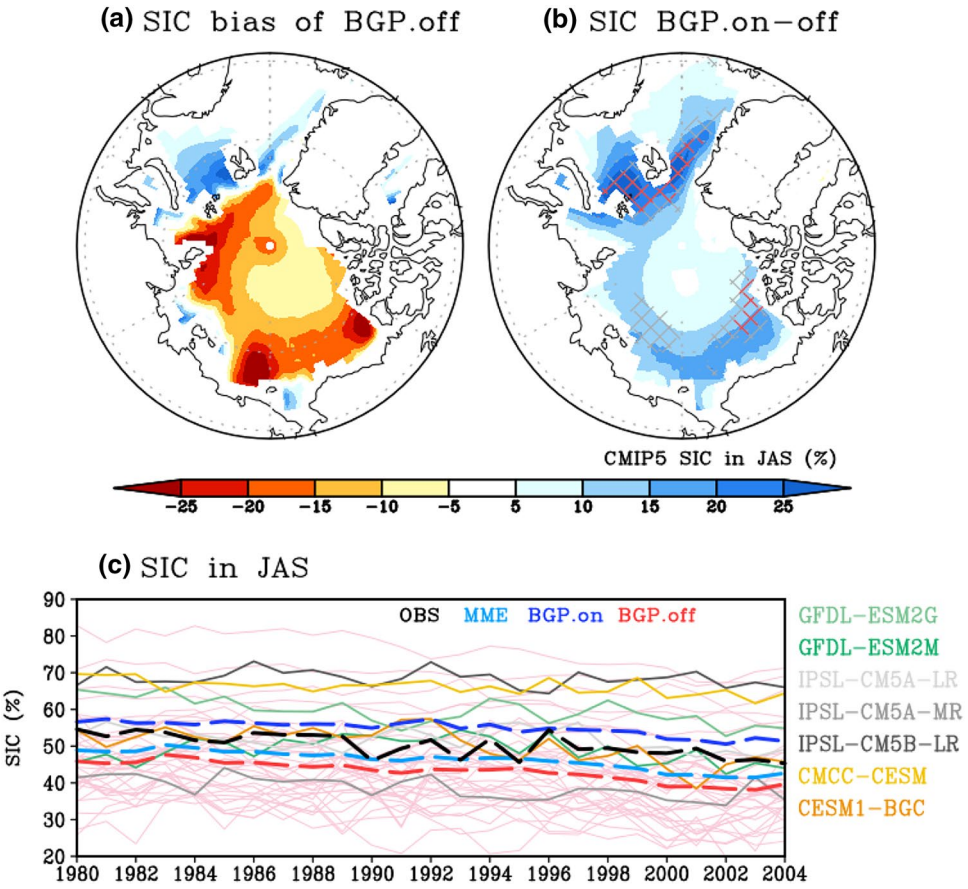

Fig. 10 **a** SIC bias of the group excluding the biogeophysical feedback (BGP.off) of CMIP5 compared with the HadISST SIC averaged from July to September (JAS). **b** SIC difference between BGP.on and BGP.off in JAS. The gray and red hatches denote the statistical significance at 90% and 95% confidence levels calculated by the Monte Carlo methodology, which randomly selected sample differences between 7 and 36 models in 10,000 times. **c** In JAS, the time series of the HadISST SIC (dashed black), the CMIP5 43 multi-model ensemble (MME; dashed sky blue), the MME of seven models of BGP.on (dashed blue), the MME of 36 models of BGP.off (dashed red), each individual model of BGP.on (green, gray, and yellow), and each model of BGP.off (light red) are shown. All groups and the CMIP5 individual model are as described in Table 2

Acknowledgements This work is supported by the project titled '[Korea-Arctic Ocean Observing System (K-AOOS), KOPRI, 20160245]', funded by the MOF, Korea, and the National Research Foundation of Korea (NRF-2017R1A2B3011511). H.-G. Lim is supported by Hyundai Motor Chung Mong-Koo Foundation.

References

Ardyna M, Babin M, Gosselin M, Devred E, Rainville L, Tremblay J (2014) Recent Arctic Ocean sea ice loss triggers novel fall phytoplankton blooms. Geophys Res Lett 41:6207–6212

Arrigo KR, van Dijken G, Pabi S (2008) Impact of a shrinking Arctic ice cover on marine primary production. Geophys Res Lett. https://doi.org/10.1029/2008gl035028

Arrigo KR, Perovich DK, Pickart RS, Brown ZW, Van Dijken GL, Lowry KE, Mills MM, Palmer MA, Balch WM, Bahr F (2012) Massive phytoplankton blooms under Arctic sea ice. Science 336:1408–1408

Arrigo KR, Perovich DK, Pickart RS, Brown ZW, van Dijken GL, Lowry KE, Mills MM, Palmer MA, Balch WM, Bates NR, Benitez-Nelson CR, Brownlee E, Frey KE, Laney SR, Mathis J, Matsuoka A, Greg Mitchell B, Moore GWK, Reynolds RA, Sosik HM, Swift JH (2014) Phytoplankton blooms beneath the sea ice in the Chukchi sea. Deep Sea Res Part II 105:1–16. https://doi.org/10.1016/j.dsr2.2014.03.018

Bhatt US, Walker DA, Walsh JE, Carmack EC, Frey KE, Meier WN, Moore SE, Parmentier F-JW, Post E, Romanovsky VE, Simpson WR (2014) Implications of Arctic Sea Ice decline for the earth system. Annu Rev Environ Resour 39:57–89. https://doi.org/10.1146/annurev-environ-122012-094357

Bintanja R, Graversen R, Hazeleger W (2011) Arctic winter warming amplified by the thermal inversion and consequent low infrared cooling to space. Nat Geosci 4:758–761

Boé J, Hall A, Qu X (2009) September sea-ice cover in the Arctic Ocean projected to vanish by 2100. Nat Geosci 2:341. https://doi.org/10.1038/ngeo467

Cabré A, Marinov I, Leung S (2015) Consistent global responses of marine ecosystems to future climate change across the IPCC AR5 earth system models. Clim Dyn 45:1253–1280

Carmack E, Barber D, Christensen J, Macdonald R, Rudels B, Sakshaug E (2006) Climate variability and physical forcing of the food webs and the carbon budget on panarctic shelves. Prog Oceanogr 71:145–181. https://doi.org/10.1016/j.pocean.2006.10.005

Ding Q, Schweiger A, Lheureux M, Battisti DS, Po-Chedley S, Johnson NC, Blanchard-Wrigglesworth E, Harnos K, Zhang Q, Eastman R, Steig EJ (2017) Influence of high-latitude atmospheric circulation changes on summertime Arctic sea ice. Nat Clim Change 7:289–295. https://doi.org/10.1038/nclimate3241. http://www.nature.com/nclimate/journal/v7/n4/abs/nclimate3241.html#supplementary-information

Dufresne J-L, Foujols M-A, Denvil S, Caubel A, Marti O, Aumont O, Balkanski Y, Bekki S, Bellenger H, Benshila R, Bony S, Bopp L, Braconnot P, Brockmann P, Cadule P, Cheruy F, Codron F, Cozic A, Cugnet D, de Noblet N, Duvel J-P, Ethé C, Fairhead L, Fichefet T, Flavoni S, Friedlingstein P, Grandpeix J-Y, Guez L, Guilyardi E, Hauglustaine D, Hourdin F, Idelkadi A, Ghattas J, Joussaume S, Kageyama M, Krinner G, Labetoulle S, Lahellec A, Lefebvre M-P, Lefevre F, Levy C, Li ZX, Lloyd J, Lott F, Madec

G, Mancip M, Marchand M, Masson S, Meurdesoif Y, Mignot J, Musat I, Parouty S, Polcher J, Rio C, Schulz M, Swingedouw D, Szopa S, Talandier C, Terray P, Viovy N, Vuichard N (2013) Climate change projections using the IPSL-CM5 earth system model: from CMIP3 to CMIP5. Clim Dyn 40:2123–2165. https://doi.org/10.1007/s00382-012-1636-1

Dunne JP, John JG, Adcroft AJ, Griffies SM, Hallberg RW, Shevliakova E, Stouffer RJ, Cooke W, Dunne KA, Harrison MJ, Krasting JP, Malyshev SL, Milly PCD, Phillipps PJ, Sentman LT, Samuels BL, Spelman MJ, Winton M, Wittenberg AT, Zadeh N (2012) GFDL's ESM2 global coupled climate–carbon earth system models. Part I: Physical formulation and baseline simulation characteristics. J Clim 25:6646–6665. https://doi.org/10.1175/jcli-d-11-00560.1

Dunne JP, John JG, Shevliakova E, Stouffer RJ, Krasting JP, Malyshev SL, Milly PCD, Sentman LT, Adcroft AJ, Cooke W, Dunne KA, Griffies SM, Hallberg RW, Harrison MJ, Levy H, Wittenberg AT, Phillips PJ, Zadeh N (2013) GFDL's ESM2 global coupled climate—carbon earth system models. Part II: Carbon system formulation and baseline simulation characteristics*. J Clim 26:2247–2267. https://doi.org/10.1175/jcli-d-12-00150.1

Griffies SM (2012) Elements of the modular ocean model (MOM). NOAA Geophysical Fluid Dynamics Laboratory, Princeton

Holland MM, Serreze MC, Stroeve J (2010) The sea ice mass budget of the Arctic and its future change as simulated by coupled climate models. Clim Dyn 34:185–200

Horvat C, Jones DR, Iams S, Schroeder D, Flocco D, Feltham D (2017) The frequency and extent of sub-ice phytoplankton blooms in the Arctic Ocean. Sci Adv. https://doi.org/10.1126/sciadv.1601191

Jerlove NG (1968) Optical oceanography. Elsevier, Oxford

Jochum M, Yeager S, Lindsay K, Moore K, Murtugudde R (2010) Quantification of the feedback between phytoplankton and ENSO in the community climate system model. J Clim 23:2916–2925

Kang X, Zhang R-H, Gao C, Zhu J (2017) An improved ENSO simulation by representing chlorophyll-induced climate feedback in the NCAR community earth system model. Sci Rep 7:17123. https://doi.org/10.1038/s41598-017-17390-2

Laufkötter C, Vogt M, Gruber N, Aita-Noguchi M, Aumont O, Bopp L, Buitenhuis E, Doney SC, Dunne J, Hashioka T, Hauck J, Hirata T, John J, Le Quéré C, Lima ID, Nakano H, Seferian R, Totterdell I, Vichi M, Völker C (2015) Drivers and uncertainties of future global marine primary production in marine ecosystem models. Biogeosciences 12:6955–6984. https://doi.org/10.5194/bg-12-6955-2015

Lee K-W, Yeh S-W, Kug J-S, Park J-Y (2014) Ocean chlorophyll response to two types of El Niño events in an ocean–biogeochemical coupled model. J Geophys Res Oceans 119:933–952. https://doi.org/10.1002/2013JC009050

Lengaigne M, Menkes C, Aumont O, Gorgues T, Bopp L, André J-M, Madec G (2007) Influence of the oceanic biology on the tropical Pacific climate in a coupled general circulation model. Clim Dyn 28:503–516. https://doi.org/10.1007/s00382-006-0200-2

Lengaigne M, Madec G, Bopp L, Menkes C, Aumont O, Cadule P (2009) Bio-physical feedbacks in the Arctic Ocean using an Earth system model. Geophys Res Lett 36:21

Lim H-G, Park J-Y, Kug J-S (2017) Impact of chlorophyll bias on the tropical Pacific mean climate in an earth system model. Clim Dyn. https://doi.org/10.1007/s00382-017-4036-8

Lindsay K, Bonan GB, Doney SC, Hoffman FM, Lawrence DM, Long MC, Mahowald NM, Moore JK, Randerson JT, Thornton PE (2014) Preindustrial-control and twentieth-century carbon cycle experiments with the earth system model CESM1(BGC). J Clim 27:8981–9005. https://doi.org/10.1175/jcli-d-12-00565.1

Manizza M, Le Quéré C, Watson AJ, Buitenhuis ET (2005) Bio-optical feedbacks among phytoplankton, upper ocean physics and sea-ice in a global model. Geophys Res Lett 32:L05603. https://doi.org/10.1029/2004GL020778

Marzeion B, Timmermann A, Murtugudde R, Jin F-F (2005) Biophysical feedbacks in the tropical Pacific. J Clim 18:58–70

Mignot J, Swingedouw D, Deshayes J, Marti O, Talandier C, Séférian R, Lengaigne M, Madec G (2013) On the evolution of the oceanic component of the IPSL climate models from CMIP3 to CMIP5: a mean state comparison. Ocean Model 72:167–184

Morel A (1988) Optical modeling of the upper ocean in relation to its biogenous matter content (case I waters). J Geophys Res 93:749–810

Morel A, Antoine D (1994) Heating rate within the upper ocean in relation to its bio-optical state. J Phys Oceanogr 24:1652–1665

Müller D, Krasemann H, Brewin RJW, Brockmann C, Deschamps P-Y, Doerffer R, Fomferra N, Franz BA, Grant MG, Groom SB, Mélin F, Platt T, Regner P, Sathyendranath S, Steinmetz F, Swinton J (2015) The ocean colour climate change initiative: I. A methodology for assessing atmospheric correction processors based on in-situ measurements. Remote Sens Environ 162:242–256. https://doi.org/10.1016/j.rse.2013.11.026

Murtugudde R, Beauchamp J, McClain CR, Lewis M, Busalacchi AJ (2002) Effects of penetrative radiation on the upper tropical ocean circulation. J Clim 15:470–486

Ohlmann JC (2003) Ocean radiant heating in climate models. J Clim 16:1337–1351. https://doi.org/10.1175/1520-0442-16.9.1337

Park J-Y, Kug J-S (2013) Marine biological feedback associated with Indian Ocean Dipole in a coupled ocean/biogeochemical model. Clim Dyn 42:329–343. https://doi.org/10.1007/s00382-012-1640-5

Park J-Y, Kug J-S, Park Y-G (2014a) An exploratory modeling study on bio-physical processes associated with ENSO. Prog Oceanogr 124:28–41. https://doi.org/10.1016/j.pocean.2014.03.013

Park J-Y, Kug J-S, Seo H, Bader J (2014b) Impact of bio-physical feedbacks on the tropical climate in coupled and uncoupled GCMs. Clim Dyn 43:1811–1827. https://doi.org/10.1007/s00382-013-2009-0

Park JY, Kug JS, Badera J, Rolph R, Kwon M (2015) Amplified Arctic warming by phytoplankton under greenhouse warming. Proc Natl Acad Sci USA 112:5921–5926. https://doi.org/10.1073/pnas.1416884112

Patara L, Vichi M, Masina S, Fogli PG, Manzini E (2012) Global response to solar radiation absorbed by phytoplankton in a coupled climate model. Clim Dyn 39:1951–1968. https://doi.org/10.1007/s00382-012-1300-9

Paulson CA, Simpson JJ (1977) Irradiance measurements in the upper ocean. J Phys Oceanogr 7:952–956

Peralta-Ferriz C, Woodgate RA (2015) Seasonal and interannual variability of pan-Arctic surface mixed layer properties from 1979 to 2012 from hydrographic data, and the dominance of stratification for multiyear mixed layer depth shoaling. Prog Oceanogr 134:19–53. https://doi.org/10.1016/j.pocean.2014.12.005

Perovich DK, Light B, Eicken H, Jones KF, Runciman K, Nghiem SV (2007) Increasing solar heating of the Arctic Ocean and adjacent seas, 1979–2005: attribution and role in the ice–albedo feedback. Geophys Res Lett 34:19

Popova EE, Yool A, Coward AC, Dupont F, Deal C, Elliott S, Hunke E, Jin M, Steele M, Zhang J (2012) What controls primary production in the Arctic Ocean? Results from an intercomparison of five general circulation models with biogeochemistry. J Geophys Res Oceans 117:C00D12. https://doi.org/10.1029/2011JC007112

Rayner N, Parker DE, Horton E, Folland C, Alexander L, Rowell D, Kent E, Kaplan A (2003) Global analyses of sea surface temperature, sea ice, and night marine air temperature since the late nineteenth century. J Geophys Res Atmos 108:D14

Sathyendranath S, Platt T (1991) Estimation of new production in the ocean by compound remote sensing. Nature 353:129

Serreze MC, Francis JA (2006) The Arctic amplification debate. Clim Change 76:241–264

Stroeve JC, Kattsov V, Barrett A, Serreze M, Pavlova T, Holland M, Meier WN (2012) Trends in Arctic sea ice extent from CMIP5, CMIP3 and observations. Geophys Res Lett 39:L16502. https://doi.org/10.1029/2012GL052676

Strutton PG, Chavez FP (2004) Biological heating in the equatorial Pacific: observed variability and potential for real-time calculation. J Clim 17:1097–1109

Timmermann A, Jin F-F (2002) Phytoplankton influences on tropical climate. Geophys Res Lett 29:19. https://doi.org/10.1029/2002gl015434

Vancoppenolle M, Bopp L, Madec G, Dunne J, Ilyina T, Halloran PR, Steiner N (2013) Future Arctic Ocean primary productivity from CMIP5 simulations: uncertain outcome, but consistent mechanisms. Glob Biogeochem Cycles 27:605–619. https://doi.org/10.1002/gbc.20055

Vichi M, Pinardi N, Masina S (2007) A generalized model of pelagic biogeochemistry for the global ocean ecosystem. Part I: Theory. J Mar Syst 64:89–109

Wassmann P, Reigstad M (2011) Future Arctic Ocean seasonal ice zones and implications for pelagic–benthic coupling. Oceanography 24(3):220–231

Yeh S-W, Kug J-S, An S-I (2014) Recent progress on two types of El Niño: observations, dynamics, and future changes. Asia Pac J Atmos Sci 50:69–81. https://doi.org/10.1007/s13143-014-0028-3

Yim BY, Min HS, Kim BM, Jeong JH, Kug JS (2016) Sensitivity of Arctic warming to sea ice concentration. J Geophys Res Atmos 121:6927–6942